COMMUNICATION

Dalton
www.rsc.org/dalton

Metallomesogens with extended bent tridentate receptors: columnar and cubic mesomorphism tuned by the size of the lanthanide metal ions †

Emmanuel Terazzi,[a] Jean-Marc Bénech,[a] Jean-Pierre Rivera,[a] Gérald Bernardinelli,[b] Bertrand Donnio,[c] Daniel Guillon[c] and Claude Piguet*[a]

[a] *Department of Inorganic, Analytical and Applied Chemistry, University of Geneva, 30 quai E. Ansermet, CH-1211 Geneva 4, Switzerland. E-mail: Claude.Piguet@chiam.unige.ch*

[b] *Laboratory of X-ray crystallography, University of Geneva, 24 quai E. Ansermet, CH-1211 Geneva 4, Switzerland*

[c] *Institut de Physique et de Chimie des Matériaux de Strasbourg, Groupe des Matériaux Organiques, 23 rue du Loess, F-67037 Strasbourg Cedex, France*

Received 4th December 2002, Accepted 24th January 2003
First published as an Advance Article on the web 3rd February 2003

The increase of the curvature of the interface between the rigid mesogenic core and the aliphatic chains in the hexacatenar tridentate ligand L3 overcomes the considerable expansion brought by the complexation of bulky metallic cores, thus leading to organized cubic mesophases for monometallic zinc^{II} and lanthanide^{III} complexes.

Although the peculiar magnetic, spectroscopic and optical properties associated with the $4f^n$ open-shell electronic configurations of trivalent lanthanides, Ln^{III}, have been exploited for the design of sophisticated molecular functional devices,[1] their introduction into macroscopic thermotropic liquid crystalline phases exhibiting novel tuneable properties remains limited.[2] A few *tetradentate* macrocyclic phthalocyanines, porphyrins and [Cu(salen)] platforms[3] provide rigid disk-shape lanthanide complexes compatible with columnar mesomorphism, while *monodentate* zwitterionic and *bidentate* aromatic salicylaldimine ligands have been developed for the preparation of lanthanide-containing calamitic mesophases.[2,4] To date, attempts to use aromatic *tridentate* binding units for generating lanthanide-containing mesophases have failed,[2] although the meridional tri-co-ordination of ligands analogous to 2,2′:6′,2″ terpyridine have been often used for extracting $Ln(NO_3)_3$ from intricate mixtures.[5] The major drawback concerns the tridentate aromatic bent core which does not match the classical molecular geometrical criteria required for calamitic (rodlike) and columnar (disclike) mesomorphism,[6] but various novel mesophase morphologies have been recently evidenced for closely related 'banana'-shaped rigid aromatic cores.[7] In this context, the introduction of extended semi-rigid lipophilic side arms at the 5,5′-positions of the bent tridentate 2,6-bis(1-alkylbenzimidazol-2-yl)pyridine binding unit transforms L1 into the extended *I-shape* receptor L2 which exhibits calamitic mesomorphism, while substitution at the 6,6′-positions produces the *V-shape* receptor L5 which displays columnar mesomorphism.[8] Although the *trans–trans* ⟶ *cis–cis* conformational change of the tridentate aromatic binding unit occurring upon complexation in $[Ln(Li)(NO_3)_3]$ (i = 1, 2, 4, 5) interconverts I-shape and V-shape arrangements which are both compatible with liquid crystalline behaviour (Scheme 1), the perpendicular expansion brought by the $Ln(NO_3)_3$ core prevents mesomorphism in the complexes.[8] In this communication, we report on (i) the first preparation of metallomesogens (*i.e.* metal-containing liquid crystals) with bent tridentate receptors derived from L1 and (ii) the first characterization of organized cubic mesophases with lanthanide complexes.

In order to unravel the consequences of reducing the size of the metallic core on the mesomorphism, L1, L2 and L4 have been reacted with $Zn(NO_3)_2{\cdot}6H_2O$ to give 72–80% yields of the complexes $[Zn(L1)(NO_3)_2]{\cdot}DMF$ (**1**) and $[Zn(Li)(NO_3)_2]{\cdot}3H_2O$ (i = 2: **2**; i = 4: **3**, see ESI). † The crystal structure of **1** ‡ shows a neutral complex $[Zn(L1)(NO_3)_2]$ and a non-interacting DMF molecule. Zn^{II} is five-coordinated in a distorted trigonal bipyramidal (tbp) arrangement made of the three nitrogen atoms of the almost planar tridentate receptor (pyridine–benzimidazole dihedral angles: 0.8 and 5.5°) and two oxygen atoms of the two monodentate co-ordinated nitrate groups (Fig. 1). The pyridine nitrogen atom N1 and the oxygen atoms O1a and O1b form the intermediate plane of the bipyramid which also contains Zn^{II} [deviation: 0.012(1) Å], while the benzimidazole nitrogens N2 and N4 occupy the apical positions. The bond angles significantly deviate from those expected for an ideal tbp geometry (Table S1, ESI †), but the ZnN_3O_2 metallic core remains significantly smaller than the nine-coordinate LuN_3O_6 core observed in the crystal structures of [Lu(L4-C1)$(NO_3)_3$] and [Lu(L2)$(NO_3)_3$].[8] Interestingly, the monodentate co-ordinated nitrate anions in $[Zn(L1)(NO_3)_2]$ are not involved in intermolecular interactions, but the aromatic benzimidazole and pyridine rings of one complex display strong π-stacking interactions with three neighbouring molecules, a crucial point for inducing long-range order in thermotropic mesophases (Fig. S1, ESI †).[8]

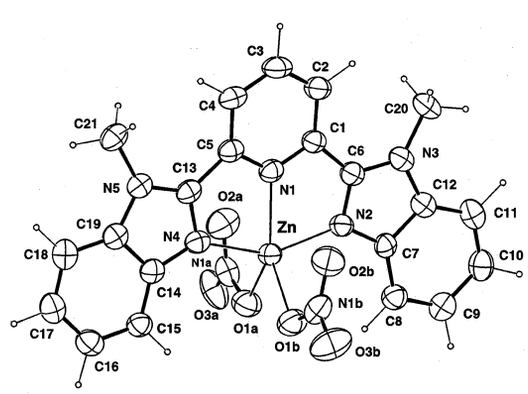

Fig. 1 Perspective view of $[Zn(L1)(NO_3)_2]$ in the crystal of **1** with ellipsoids represented at the 40% probability level.

† Electronic supplementary information (ESI) available: experimental procedures and characterization (elemental analyses, NMR, ESI-MS, conductivity) for L3, L3-C4 and L4 and for the complexes $[Zn(L1)(NO_3)_2]{\cdot}DMF$ (**1**), $[Zn(Li)(NO_3)_2]{\cdot}3H_2O$ (i = 2: **2**; i = 4: **3**), $[Zn(L3)(NO_3)_2]{\cdot}H_2O$ (**4**) and $[Ln(L3)(NO_3)_3]$ (Ln = Eu, **5**; Ln = Dy, **6**; Ln = Lu, **7**). Tables collecting selected bond distances and bite angles for **1** and L3-C4 and scattering vectors for **5**–**7**. Figures showing intermolecular interactions in **1** and L3-C4, DSC traces for **2**, **4** and **6**, birefringent textures for L3 and **7** and a CPK modeling for **7**. See http://www.rsc.org/suppdata/dt/b2/b211902a/

DOI: 10.1039/b211902a

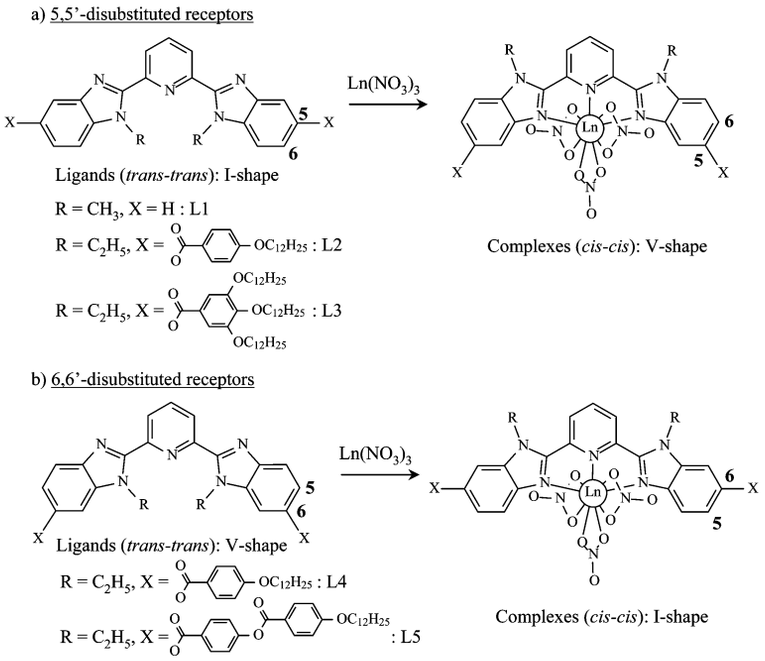

Scheme 1 Conformational changes (*trans–trans* ⟶ *cis–cis*) occurring upon complexation to Ln^{III} and associated molecular anisometries observed for L1–L5.

The similarity of the ν(CN) and $\nu(NO_2)$ vibrations assigned to the co-ordinated tridentate aromatic receptor and to the monodentate nitrate groups in the IR spectra of **1**–**3**, points to the existence of comparable five-coordinate ZnN_3O_2 metallic cores in the three complexes. A combination of thermogravimetric analysis (TGA), differential scanning calorimetry (DSC) and polarizing optical microscopy shows that the I-shape complex $[Zn(L4)(NO_3)_2]\cdot 3H_2O$ (**3**) displays no mesomorphism, but the V-shape complex $[Zn(L2)(NO_3)_2]\cdot 3H_2O$ (**2**) exhibits a monotropic birefringent mesophase at 251 °C followed by decomposition occurring at 254 °C (two water molecules are lost in the 200–240 °C range, Table 1 and Fig. S2, ESI†). Although fast decomposition occurring in the mesophase limits further characterization, the poorly developed focal-conic fan texture suggests (i) a smectogenic behaviour and (ii) that V-shape 5,5′-disubstituted receptors coordinated to $Zn(NO_3)_2$ are compatible with the formation of metallomesogens.

Since an increase of the volume fraction of the alkyl chains favours the formation of stable and organized columnar or cubic mesophases at low temperatures,[7,9,10] we have synthesized the 5,5′-disubstituted hexacatenar receptor L3† in which the aromatic–aliphatic interface curvature is no more planar. The crystal structure of the L3-C4§ derivative in which the dodecyloxy chains are replaced with butyloxy chains, reveals the phasmidic shape of the receptor resulting from the connection of six divergent flexible alkyloxy chains to the central I-shape aromatic core (Fig. 2). The bent tridentate binding unit adopts the expected *trans–trans* conformation, but significant torsions between the connected aromatic groups (interplanar angles 30.1–53.3°) produce a helical twist along the ligand strand which limits intermolecular interactions to a single π-stacking observed between adjacent benzimidazole rings (Fig. S3, ESI†).

L3 exhibits columnar mesomorphism at room temperature (Cr 25 Col 63 I) as indicated by its characteristic fan texture observed by polarizing microscopy (Table 1 and Fig. S4, ESI†).[11] Complexation of L3 with $Zn(NO_3)_2\cdot 6H_2O$ gives 81% of $[Zn(L3)(NO_3)_2]\cdot H_2O$ (**4**)† whose IR spectrum is reminiscent to those observed for complexes **1**–**3**, thus pointing to the formation of a similar five-coordinate ZnN_3O_2 core. The DSC trace shows that the crystals melts at 122 °C to give a highly viscous bicontinuous cubic mesophase characterized by its isotropic texture (no optical texture is observed under the polarizing microscope, except for the generation of geometric bright birefringent flashes obtained upon abrupt mechanical constraints, Table 1 and Fig. S5, ESI†). Decomposition occurs at 195 °C, but the impressive stabilization of the mesophase observed when going from $[Zn(L2)(NO_3)_2]$ (**2**, melting point:

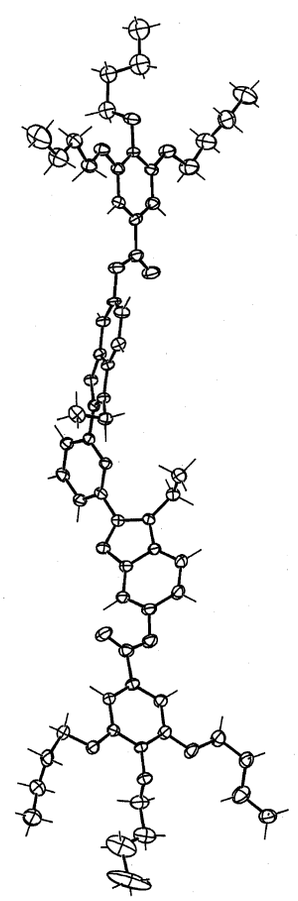

Fig. 2 Perspective view of the hexacatenar ligand L3-C4 with ellipsoids represented at the 40% probability level.

Table 1 Phase-transition temperatures and enthalpy and entropy changes for ligands L2–L4 and for the complexes $[Zn(L2)(NO_3)_2]\cdot 3H_2O$ (**2**), $[Zn(L4)(NO_3)_2]\cdot 3H_2O$ (**3**), $[Zn(L3)(NO_3)_2]\cdot H_2O$ (**4**) and $[Ln(L3)(NO_3)_3]$ (Ln = Eu, **5**; Ln = Dy, **6**; Ln = Lu, **7**)

Compound	Transition[a]	T/°C	ΔH/kJ mol^{-1}	ΔS/J mol^{-1} K^{-1}
L2[b]	Cr–SmC	131	35	86
	SmC–SmA	217		
	SmA–N	223		
	N–I	226	7	14
$[Zn(L2)(NO_3)_2]\cdot 3H_2O$ (**2**)	Cr–Cr′	114	3	7
	Loss of two H_2O	120–240	13	28
	Cr′–SmX	251	14	27
	SmX dec.	254		
L4	Cr–I	172	34	76
$[Zn(L4)(NO_3)_2]\cdot 3H_2O$ (**3**)	Cr–Cr′	39	21	68
	Cr′–Cr″	232	41	81
	Dec.	306		
L3	Cr–Col	25[c]		
	Col–I	63	3	10
$[Zn(L3)(NO_3)_2]\cdot H_2O$ (**4**)	Cr–Cr′	23	43	137
	Cr′–Cub_v	122	43	108
	Cub_v dec.	195		
$[Eu(L3)(NO_3)_3]$ (**5**)	Cr–Cr′	8–35[d]	45	
	Cr′–Cub_v	134	36	87
	Cub_v dec.	188		
$[Dy(L3)(NO_3)_3]$ (**6**)	Cr–Cr′	4–32[d]	50	
	Cr′–Cub_v	151	40	95
	Cub_v dec.	204		
$[Lu(L3)(NO_3)_3]$ (**7**)	Cr–Cr′	19	20	68
	Cr′–Col_h	157	37	86
	Col_h dec.	217		

[a] Cr = Crystal, SmC = smectic C phase, SmA = smectic A phase, SmX = undetermined smectic phase, N = nematic phase, Col_h = hexagonal columnar phase, Cub_v = bicontinuous cubic phase, I = isotropic fluid, dec. = decomposition; temperatures are given as the onset of the peak observed during heating processes (Seiko DSC 220C differential scanning calorimeter, 5 °C min^{-1}, under N_2); the liquid crystalline phases were identified from their optical textures and from XRD studies. [b] According to ref. 8. [c] Second-order vitrous transition determined by optical polarizing microscopy. [d] Several closely spaced Cr–Cr′ transitions for which only the total enthalpic change is reported.

251 °C) to $[Zn(L3)(NO_3)_2]$ (**4**, melting point 122 °C) may be assigned to the increased curvature of the aromatic–aliphatic interface with L3.[6,7] Reaction of L3 with the bulky $Ln(NO_3)_3\cdot nH_2O$ cores (Ln = Eu, Dy, Lu) give 87–92% yields of $[Ln(L3)(NO_3)_3]$ (Ln = Eu, **5**; Ln = Dy, **6**; Ln = Lu, **7**).† Although no crystal structure could be obtained for **5**–**7** (or derivatives of them), the similarity of their IR spectra with those reported for the analogous complexes $[Lu(L4\text{-}C1)(NO_3)_3]$ and $[Lu(L2)(NO_3)_3]$[8] for which the crystal structures show distorted nine-coordinated Lu^{III} (three N-atoms of the tridentate receptor and six O-atoms of three bidentate nitrate groups, Scheme 1), implies that closely related LnN_3O_6 metallic cores occur in **5**–**7**. The DSC traces of **5**–**7** are similar and display a single melting transition occurring at 134, 151 and 157 °C for Ln = Eu, Dy and Lu respectively. The clearing temperatures of the highly viscous mesophases could not be determined due to the thermal degradation of the complexes at 188, 204 and 217 °C (Table 1, Fig. S6, ESI†). Isotropic textures, typical of cubic mesophases, are observed for Ln = Eu and Dy by polarizing microscopy, and up to seven fine reflexions observed by X-ray diffraction at 165–170 °C for $[Ln(L3)(NO_3)_3]$ (Ln = Eu, **5**; Ln = Dy, **6**) and corresponding to the squared spacing ratios 2, 4, 6, 8, 10, 12, 14 confirm the formation of body-centred cubic lattices[10] with a = 38.0 Å (Ln = Eu) and a = 37.9 Å (Ln = Dy) (Tables S2–S3, ESI†). Taking an approximate, but realistic density of d = 1.0 g cm^{-3} in the mesophase, the number of molecules per unit cell amounts to $N = (d\cdot N_{av}\cdot a^3\cdot 10^{-24})/M_r = 16$ for **5** and **6** (N_{av} is the Avogadro number and M_r is the molecular weight of the complexes) which is compatible with the space groups $Im\bar{3}$, $Ia\bar{3}$ and $Im\bar{3}m$ which possess satisfying reflection conditions and 16 general or special Wykoff positions ($I432$ is rejected because its point group allows optical activity which is not observed for **5** and **6**). These features are compatible with the existence of a bicontinuous cubic phase (Cub_v) made of two interpenetrated networks of branched cylinders (with a connectivity 6) containing one of the incompatible molecular parts (the rigid cores) in a continuum of the other one (the packed molten paraffinic chains, characterized by a diffuse reflection at about 4.5 Å, Fig. 3).[7,9,10]

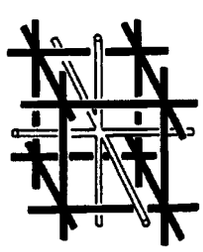

Fig. 3 Interconnecting rod model for the $Im\bar{3}m$ space group showing the two interpenetrated octahedral networks formed by the rigid part of the complexes $[Ln(L3)(NO_3)_3]$ (Ln = Eu, **5**; Ln = Dy, **6**). The chains extend to fill the space between them (adapted from ref. 9).

Interestingly, the minor contraction of the nine-coordinate metallic radius when going from Ln = Dy (r = 1.083 Å) in **6** to Ln = Lu (r = 1.032 Å) in **7** has a dramatic effect on the organization of the molecules within the mesophase. For $[Lu(L3)(NO_3)_3]$ (**7**), a birefringent texture develops under the polarizing microscope in the mesophase and seven fine reflexions are observed by X-ray diffraction at 165 °C corresponding to the squared spacing ratios 1, 3, 4, 7, 9, 12, 13, and the indexation (hk) = (10), (11), (20), (21), (30), (22), (31) (Table S4 and Fig. S7, ESI†). This pattern together with a single diffuse band at 4.5 Å indicate the formation of a hexagonal columnar arrangement (Col_h, plane groups $p6$ or $p6mm$) with an intercolumnar separation of a = 31.2 Å and a cross sectional area S = 842 Å^2. Taking a stacking period within the colums of approximately h = 4.5 Å corresponding to the thickness of a single layer (the associated diffraction peak is masked by that of the molten chains)[10] and a density of d = 1.0 g cm^{-3} in the mesophase, we calculate $N = (d\cdot N_{av}\cdot S\cdot h\cdot 10^{-24})/M_r = 1.1 \approx 1$ which strongly suggests that

a single [Lu(L3)$(NO_3)_3$] complex occupies the cross-section of the column. A rough CPK modeling of the V-shape complex [Lu(L3)$(NO_3)_3$] in its extended configuration suggests that the surface covered by the circumscribed ellipse amounts to 942 Å^2 which is only slightly larger than the observed cross-section and requires only a slight tilt of the elliptical complex in the column (Fig. S8, ESI †). In spite of their hemidisc molecular shapes and due to steric hindrance, the complexes likely stacked in an alternated fashion *i.e.* antiparallel, forming as such an overall discoid cross-section.[11]

In conclusion, these preliminary results demonstrate for the first time that (i) the increase of the curvature of the interface in the tridentate hexacatenar ligand L3 overcomes the considerable expansion brought by the complexation of bulky metallic cores, thus leading to organized cubic mesophases for zinc^{II} and lanthanide^{III} complexes and (ii) the minor contraction of the lanthanide size may induce a transition between cubic and columnar mesomorphism. The latter point is reminiscent of the undulating columnar cores model[10] which suggests that a columnar hexagonal phase can be transformed into a cubic phase when large oscillation amplitudes are induced within the columns. The replacement of the small Lu^{III} ion with the larger Eu^{III} and Dy^{III} ions in [Ln(L3)$(NO_3)_3$] seems to be sufficient for inducing such structural variations.

Financial support from the Swiss National Science Foundation, National Research Programme 47 'Supramolecular Functional Materials' is gratefully acknowledged.

Notes and references

‡ Crystal data for **1**: [$(C_{21}H_{17}N_5)Zn(NO_3)_2$]$(C_3H_7NO)$, M_r = 601.9, T = 200 K, monoclinic, $P2_1/c$, Z = 4, a = 9.6975(5), b = 13.3453(6), c = 20.2749(11) Å, β = 96.930(6)°, V = 2604.7(3) Å^3. 20743 measured reflections, 5081 unique reflections (R_{int} = 0.047), R = 0.036, ωR = 0.038 for 361 variables and 3253 contributing reflections [$|F_o| > 4\sigma(F_o)$]. CCDC reference number 194452.

§ Crystal data for L3-C4: $C_{61}H_{77}N_5O_{10}$, M_r = 1040.4, T = 200 K, triclinic, $P\bar{1}$, Z = 2, a = 12.5210(9), b = 14.7685(11), c = 17.6867(12) Å, a = 113.831(3), β = 91.239(8), γ = 101.452(9)°, V = 2913.2(4) Å^3. 23214 measured reflections, 10651 unique reflections (R_{int} = 0.078), $R = \omega R$ = 0.049 for 680 variables and 4003 contributing reflections [$|F_o| > 4\sigma(F_o)$]. One of the butyl chains was disordered (C26–C29) and refined on two different sites (PP = 0.6 : 0.4) with isotropic atomic displacement parameters. CCDC reference number 194451. See http://www.rsc.org/suppdata/dt/b2/b211902a/ for crystallographic data in CIF or other electronic format.

1 (*a*) D. Parker, R. S. Dickins, H. Puschmann, C. Crossland and J. A. K. Howard, *Chem. Rev.*, 2002, **102**, 1977; (*b*) J.-C. G. Bünzli and C. Piguet, *Chem. Rev.*, 2002, **102**, 1897.
2 For a comprehensive recent review, see K. Binnemans and C. Görller-Walrand, *Chem. Rev.*, 2002, **102**, 2303.
3 (*a*) C. Piechocki, J. Simon, J. J. André, D. Guillon, P. Petit, A. Skoulios and P. Weber, *Chem. Phys. Lett.*, 1985, **122**, 124; (*b*) H. Miwa, N. Kobayashi, K. Ban and K. Ohta, *Bull. Chem. Soc. Jpn.*, 1999, **72**, 765; (*c*) K. Binnemans, K. Lodewyckx, B. Donnio and D. Guillon, *Chem. Eur. J.*, 2002, **8**, 1101.
4 K. Binnemans, Y. G. Galyametdinov, R. Van Deun, D. W. Bruce, S. R. Collinson, A. P. Polishchuk, I. Bikchantaev, W. Haase, A. V. Prosvirin, L. Tinchurina, U. Litvinov, A. Gubajdullin, A. Rakhmatullin, K. Uytterhoeven and L. Van Meervelt, *J. Am. Chem. Soc.*, 2000, **122**, 4335.
5 (*a*) M. G. B. Drew, M. J. Hudson, P. B. Iveson, C. Madic and M. L. Russel, *J. Chem. Soc., Dalton Trans.*, 2000, 2711; (*b*) M. G. B. Drew, P. B. Iveson, M. J. Hudson, J. O. Liljenzin, L. Spjuth, P.-Y. Cordier, A. Enarsson, C. Hill and C. Madic, *J. Chem. Soc., Dalton Trans.*, 2000, 821.
6 (*a*) B. Donnio and D. W. Bruce, *Struct. Bonding (Berlin)*, 1999, **95**, 193; (*b*) C. Tschierske, *Angew. Chem., Int. Ed.*, 2000, **39**, 2454; (*c*) R. Ziessel, L. Douce, A. El-ghayoury, A. Harriman and A. Skoulios, *Angew. Chem., Int. Ed.*, 2000, **39**, 1489.
7 (*a*) G. Pelzl, S. Diele and W. Weissflog, *Adv. Mater.*, 1999, **11**, 707; (*b*) C. Tschierske, *J. Mater. Chem.*, 2001, **11**, 2647.
8 (*a*) H. Nozary, C. Piguet, P. Tissot, G. Bernardinelli, J.-C. G. Bünzli, R. Deschenaux and D. Guillon, *J. Am. Chem. Soc.*, 1998, **120**, 12274; (*b*) H. Nozary, C. Piguet, J.-P. Rivera, P. Tissot, G. Bernardinelli, N. Vulliermet, J. Weber and J.-C. G. Bünzli, *Inorg. Chem.*, 2000, **39**, 5286; (*c*) H. Nozary, C. Piguet, J.-P. Rivera, P. Tissot, P.-Y. Morgantini, J. Weber, G. Bernardinelli, J.-C. G. Bünzli, R. Deschenaux, B. Donnio and D. Guillon, *Chem. Mater.*, 2002, **14**, 1075.
9 D. W. Bruce, *Acc. Chem. Res.*, 2000, **33**, 831.
10 B. Donnio, B. Heinrich, T. Gulik-Krzywicki, H. Delacroix, D. Guillon and D. W. Bruce, *Chem. Mater.*, 1997, **9**, 2951.
11 A. G. Serrette, C. K. Lai and T. M. Swager, *Chem. Mater.*, 1994, **6**, 2252.